

# RSC Advances



This is an *Accepted Manuscript*, which has been through the Royal Society of Chemistry peer review process and has been accepted for publication.

*Accepted Manuscripts* are published online shortly after acceptance, before technical editing, formatting and proof reading. Using this free service, authors can make their results available to the community, in citable form, before we publish the edited article. This *Accepted Manuscript* will be replaced by the edited, formatted and paginated article as soon as this is available.

You can find more information about *Accepted Manuscripts* in the [Information for Authors](#).

Please note that technical editing may introduce minor changes to the text and/or graphics, which may alter content. The journal's standard [Terms & Conditions](#) and the [Ethical guidelines](#) still apply. In no event shall the Royal Society of Chemistry be held responsible for any errors or omissions in this *Accepted Manuscript* or any consequences arising from the use of any information it contains.

# Thermal curing of novel carborane-containing phenylethynyl terminated imide oligomers

Jie Yue<sup>ab</sup>, Yuntao Li<sup>\*ab</sup>, Hui Li<sup>b</sup>, Yan Zhao<sup>c</sup>, Chunxia Zhao<sup>b</sup>, and Xiangyu Wang<sup>b</sup>

a State Key Lab of Oil and Gas Reservoir Geology and Exploitation, Southwest Petroleum University, Chengdu 610050, China.\*E-mail: yuntaoli@swpu.edu.cn; Fax: 86-28-83032852; Tel: 86-28-83032852.

b Department of Materials Science and Engineering, Southwest Petroleum University, Chengdu 610050, China.

c Department of Materials Science and Engineering, Beijing University of Aeronautics and Astronautics, Beijing 100191, China.

## Abstract

A novel carborane-containing phenylethynyl terminated imide compound (Carb-PEPA) as a modifier for fluorinated phenylethynyl terminated imide oligomer (AFR-PEPA) was synthesized and characterized by FTIR and <sup>1</sup>H-NMR. The resin systems consisting of Carb-PEPA and AFR-PEPA (AFR-PEPA-Carb) were prepared with different weight fractions of Carb-PEPA. The thermal curing kinetics and thermal stability of the imide compound and resultant resin systems were analyzed by using DSC and TGA respectively. The relevant kinetic data were determined by Kissinger method. The results show that the glass transition temperatures (T<sub>g</sub>) of the cured resin systems increase with the addition of Carb-PEPA. The imide system containing 20 wt%

Carb-PEPA (AFR-PEPA-Carb-20) exhibits the highest Tg of 389.5°C due to the high steric hindrance of carborane. The char yield of the resin was also increased with the introduction of carborane structure in the system. The kinetic data indicate that AFR-PEPA/Carb-PEPA imide blends have higher activation energy  $E$  and frequency factor  $A$  than AFR-PEPA imide oligomers.

**Keywords:** polyimide, imide oligomer, carborane, cure kinetics, thermal properties

## Introduction

High performance polyimide matrices have been developed for service at high temperature due to their excellent thermal and mechanical properties. Their composites are widely used in electronics and aerospace industries. 【1,2】

Phenylethynyl end-capped fluorinated imide oligomer and its polyimide AFR-PE developed by the U.S Air Force Research Laboratory is one of the resin matrices giving the best overall properties for aerospace composite applications. AFR-PE has a glass transition temperature of as high as 400 °C, good mechanical properties at high temperatures and durability of the muggy conditions.【3-8】 However, the degradation and aging of the matrix have restricted its further development and applications. Continuous exposure to high temperatures could cause mass loss, cracking and performance degradation. Many studies have been carried out to improve thermal stability of polyimide materials over the recent years. The previous work demonstrates that making the polymer structure organic/inorganic hybrid could effectively address the issue. 【9-14】

Iscoahedral carboranes such as o-, m-, and p-C<sub>2</sub>B<sub>10</sub>H<sub>12</sub> have great thermal and

chemical stability due to their stable cage structures and rich boron contents. The thermal stability of polymers could be greatly enhanced by the incorporation of carboranes into the matrices. Particular attention has been paid to the development of carborane-containing polymers with high thermal stability. The carborane-containing polymers, such as polysilanes, polysiloxanes and polyetherketones have been investigated as advanced materials with enhanced thermal stability. Among all of those, polymers in which the carborane cage into the main chain and pendant to the chain are two main types. 【15-20】 Generally, carboranes can be introduced into polymers via the reaction of decaborane with an existing triple bond in order to prepare the o-carborane containing compound. However, carborane-containing phenylethynyl terminated imide oligomer has not been reported in previous literatures yet.

The main aim of this work is to study the thermal curing behavior and thermal stability of carborane-containing phenylethynyl terminated imide compound (Carb-PEPA) and its blends with fluorinated phenylethynyl terminated imide oligomer (AFR-PEPA). First of all, 1-(4-aminophenyl)-2-dicarbodeaborane was synthesized and characterized. It was then used to synthesize the imide compound Carb-PEPA with 4-phenylethynyl phthalic anhydride (PEPA). Carb-PEPA was used as a modifier for AFR-PEPA. The blend of Carb-PEPA and AFR-PEPA undergoes addition reactions through triple bond  $C\equiv C$  to form a stable crosslinking network during curing process. The curing kinetic of the prepared resin systems were investigated by using differential scanning calorimetry (DSC).

## Experimental

### Materials

Decaborane was purchased from Zhengzhou Sigma Chemical Co., Ltd. (China). Para-nitrophenylacetylene was synthesized according to a reported literature. **【21】** 4,4'-(Hexafluoroisopropylidene) diphthalic anhydride (6FDA) and 4-phenylethynyl phthalic anhydride (PEPA) were purchased from Changzhou sunlight pharmaceutical. N-methylpyrrolidinone (NMP), toluene, acetonitrile, glacial acetic acid, tin (II) chloride dehydrate, 1,4-phenylenediamine (p-PDA) and methanol were provided by Chengdu Kelong Chemical Reagents Corp. (China). Solvents were dried and distilled following the standard procedures. All the reagents were used as received without further purification. The synthesis was conducted in a dry/inert atmosphere due to the high oxidizability and hygroscopicity of the raw materials.

### Synthesis of 1-(4-nitrophenyl)-2-dicarbodeaborane (Compound 1)

Decaborane (610 mg, 5 mmol) was refluxed in acetonitrile (25ml) for 3h. **【22】** The reaction mixture was cooled to room temperature (~25°C), then the para-nitrophenylacetylene (735 mg, 5 mmol) in dry acetonitrile was added to the reaction mixture. The resulting mixture was further refluxed at 90°C for 12h. The reaction mixture was then filtered through a cotton plug and concentrated. The crude product was purified by silica gel column chromatography with 10% ethyl acetate in petroleum ether as eluent to obtain the pure compound 1-(4-nitrophenyl)-2-dicarbodecaborane (yellow powder, 183.8 mg). Yield: 14%.

$^1\text{H-NMR}$  (400MHz,  $\text{CDCl}_3$ , ppm): 7.19 (d,  $J=8\text{Hz}$ , 2H), 6.51 (d,  $J=8\text{Hz}$ , 2H), 5.58 (s, H), 2.85-1.15 (m, 10H).  $^{13}\text{C-NMR}$  (100 MHz,  $\text{CDCl}_3$ , ppm): 146.90, 113.37, 128.21, 121.85, 76.01, 60.29. FTIR (KBr,  $\text{cm}^{-1}$ ): 2580, 2095, 1515, 1343.

### Synthesis of 1-(4-aminophenyl)-2-dicarbodeaborane (Compound 2)

The compound 1 (183.8 mg, 0.69 mmol) and glacial acetic acid (20ml) were added into a 250ml round-bottomed flask. Then tin (II) chloride dehydrate (1.93 g, 10.5 mmol) was slowly added into the flask with stirring. The suspension was heated to approximately  $80^\circ\text{C}$  at a heating rate of  $8^\circ\text{C}/\text{min}$ . The reaction was monitored using thin-layer chromatography. A homogeneous solution was obtained when the reaction was completed. The reaction mixture was then cooled and poured into distilled water (150ml) after stirring for 0.5h. The solution was neutralized with 20 wt% NaOH solution until the neutral litmus paper turned blue. The suspension was extracted with diethyl ether and the ethereal layer was dried over anhydrous sodium sulfate overnight. The crude product was obtained and further purified by silica gel column chromatography to prepare 1-(4-aminophenyl)-2-dicarbodeaborane (126.8 mg) after the solvent was concentrated. Yield: 78%.  $^1\text{H-NMR}$  (400MHz,  $\text{CDCl}_3$ , ppm): 7.24 (d,  $J=8\text{Hz}$ , 2H), 6.53 (d,  $J=8\text{Hz}$ , 2H), 3.82 (s, H), 2.85-1.15 (m, 10H).  $^{13}\text{C-NMR}$  (100 MHz,  $\text{CDCl}_3$ , ppm): 149.01, 114.32, 129.23, 123.52, 77.23, 61.87. FTIR (KBr,  $\text{cm}^{-1}$ ): 3472, 2593, 1618.

### Synthesis of imide compound Carb-PEPA

The carborane-containing imide compound Carb-PEPA was prepared by the

following method. The 1-(4-aminophenyl)-2-dicarbodeborane (235 mg, 1 mmol) and PEPA (248 mg, 1 mmol) were dissolved in NMP (25 ml) in a 100ml round-bottom flask equipped with a magnetic stirrer under the protection of nitrogen atmosphere. The mixture solution was reacted at room temperature for 12h and then slowly heated up to 140°C following by holding for 12h. When the reaction was completed, the reaction solution was poured into a petri dish and placed into an oven to remove the NMP. The resultant powders were dried at 180°C for 24h in vacuum. Yield: 94%. The model compound has a theoretical molecular weight of 465.6 g/mol. The chemical structure of Carb-PEPA is shown in Figure 1a.

#### **Synthesis of imide oligomer AFR-PEPA**

The imide oligomer AFR-PEPA was prepared from p-PDA, 6FDA and PEPA in NMP according to the previous literature. 【23】 The p-PDA (1.4068 g, 13 mmol) was dissolved in NMP (30 ml) under nitrogen at room temperature in a 250 ml, three-neck round-bottom flask equipped with a magnetic stirrer and a gas adaptor. The 6FDA (2.2684g, 10.4 mmol) was dissolved in 30 ml NMP under nitrogen protection. The solution of 6FDA/NMP was then added in p-PDA/NMP solution three portions over 3h. After all the 6FDA solution was added, the solution was stirred for 20h at room temperature. Then the solid PEPA (1.2918 g, 5.2 mmol) was added and stirred until completely reacted (4 hours) under nitrogen. Subsequently, toluene was added and the resulting mixture was imidized under reflux in an oil bath of 180°C with the removal of water via azeotropic distillation. The reaction mixtures were finally added into

distilled water, filtered, washed in boiling water, followed by the removal of NMP in warm methanol. Very fine yellow powders were produced and dried at 160°C for 24h. Yield: 96%. The polymerization degree of the imide oligomer is 4 and the theoretical molecular weight is 2634g/mol. The chemical structure of AFR-PEPA imide oligomer is shown in Figure 1b.

### Thermal cure of imide oligomers

Carb-PEPA was added to the AFR-PEPA with stirring using a magnetic stirrer for 10 min, followed by an ultrasonic dispersion process for another 10min in order to obtain uniformly dispersed imide blends. AFR-PEPA imide oligomers containing 10 and 20 wt% Carb-PEPA were prepared and denoted as AFR-PEPA-Carb-10 and AFR-PEPA-Carb-20 respectively.

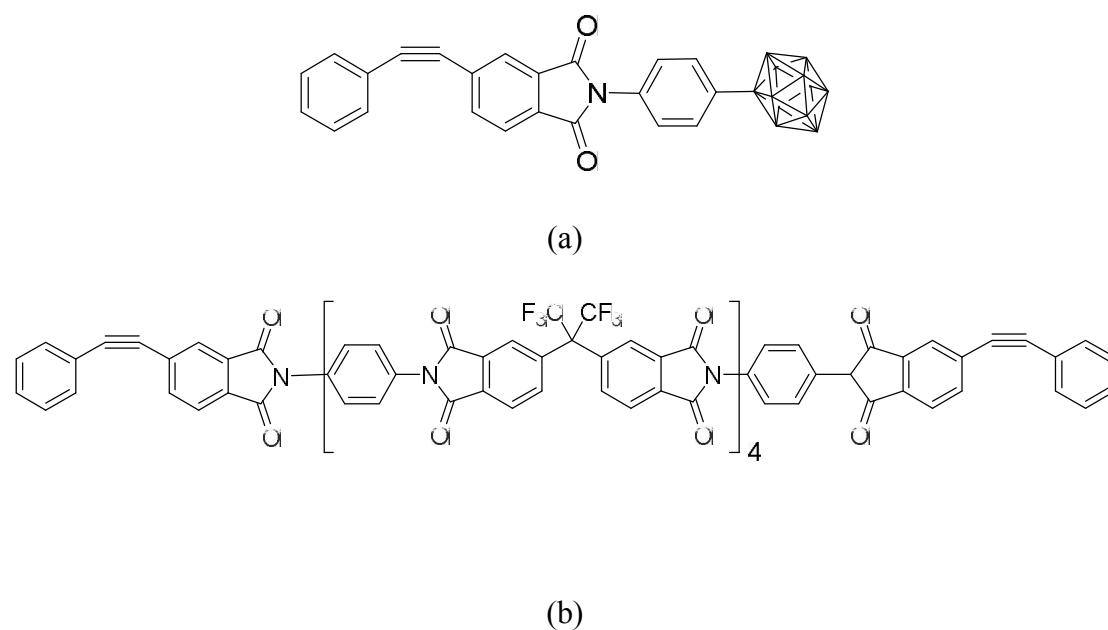


Figure 1. Chemical structure of the imide compound Carb-PEPA and imide oligomer AFR-PEPA . a. Carb-PEPA; b. AFR-PEPA



The imide blends were placed in ceramic crucibles and then heated to 380°C and held for 1h in a muffle furnace. The thermally cured polyimides were removed from the crucibles after cooling to room temperature and then characterized by FT-IR.

DSC measurement was carried out to investigate the effects of curing temperature on the curing behavior of imide blends. A dry nitrogen flow was used as purge gas at a flow rate of 50 ml/min. DSC experiments were performed with temperatures ranging from room temperature to 450 °C at various heating rates of 2.5, 5, 10, 15 and 20°C/min using a TA Q20. The curing kinetic parameters of the prepared resin systems were calculated through Kissinger and Crane methods.

## Measurements

### NMR

<sup>1</sup>H-NMR and <sup>13</sup>C-NMR spectra were recorded on a Bruker Avance III 400 spectrometer (400 MHz for <sup>1</sup>H-NMR and 100MHz for <sup>13</sup>C-NMR) by using chloroform-d as solvents and tetramethylsilane as an internal standard.

### FT-IR

Fourier transform infrared spectroscopic (FT-IR) characterization was carried out using a Nicolet 6700 spectrometer by potassium bromide (KBr) pellets.

### TGA

Thermogravimetric analysis (TGA) was carried out from room temperature to 800°C at heating rate of 20°C/min using a TGA/SDTA851e thermogravimetric analyzer

under nitrogen atmosphere.  $T_{5\%}$  and  $T_{10\%}$  represent the temperature resulting in 5% and 10% weight loss relative to the initial weight.

## DSC

Conventional DSC tests were conducted from room temperature to 450 °C at various heating rates of 2.5, 5, 10, 15, 20 °C/min using a TA Q20 module under nitrogen to investigate the effect of curing temperature on the curing behavior. The cure reaction was considered to be completed when the rate curves leveled off.

## MDSC

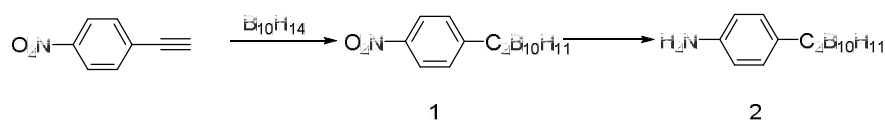
Temperature-modulated different scanning calorimetric (MDSC) was conducted from room temperature to 450 °C using a TA Q2000 apparatus equipped with temperature-modulation package under nitrogen to investigate the cure reaction of imide oligomers and  $T_g$  of cured polyimides. The MDSC tests were carried out at a ramp rate of 3°C/min and modulation amplitude of 1°C every 60s. The initial and terminal temperatures of the cure reaction on MDSC curves were used to determine the baselines and calculate the total heat of reaction.

## Results and discussion

### Characterization of 1-(4-aminophenyl)-2-dicarboabborane

The synthesis route for the desired compound 2 is illustrated in Scheme 1. The target compound was obtained via the addition and reduction reactions. FTIR,  $^1\text{H-NMR}$  and  $^{13}\text{C-NMR}$  were employed to characterize the structure of

1-(4-aminophenyl)-2-dicarbodeaborane.



Scheme 1. Synthesis route of 1-(4-aminophenyl)-2-dicarbodeaborane

The FTIR results in Figure 2 show the characteristic peaks of B-H stretching at 2593  $\text{cm}^{-1}$  for carborane-containing compound. The peaks at 2095  $\text{cm}^{-1}$ , 1515  $\text{cm}^{-1}$  and 1343  $\text{cm}^{-1}$  for para-nitrophenylacetylene, corresponding to the triple bond  $\text{C} \equiv \text{C}$ , asymmetric and symmetric N=O stretching vibration respectively, disappeared after the addition and reduction reactions. The adsorption band at 857  $\text{cm}^{-1}$  is the characteristic band of C-N stretching vibration. The presence of new peaks corresponding to the asymmetric N-H stretching vibration at 3472  $\text{cm}^{-1}$ , the symmetric N-H stretching vibration at 3414  $\text{cm}^{-1}$  and the N-H bending vibration at 1618  $\text{cm}^{-1}$ , indicates a successful reduction reaction to produce the desired compound 2.

$^1\text{H-NMR}$  and  $^{13}\text{C-NMR}$  spectra of compound 2 are shown in Figure 3. The proton peaks at 3.74 (2H;  $\text{NH}_2$ ), 7.24(2H; Ar-H), 6.53(2H; Ar-H), 3.82(H; C-H) and 1.15-2.85 (10H; B-H) ppm can be observed in Figure 3a, representing the amino groups ( $\text{NH}_2$ ), benzene ring (Ar-H) and boron cage (C-H, B-H), respectively. Six peaks at 146.90 (Ar-C), 113.37 (Ar-C), 128.21 (Ar-C), 121.85 (Ar-C), 76.01 (B-C) and 60.29 (B-C) ppm occur in the  $^{13}\text{C-NMR}$  spectrum, as shown in Figure 3b. The FTIR,  $^1\text{H-NMR}$  and  $^{13}\text{C-NMR}$  results indicate that the expected

1-(4-aminophenyl)-2-dicarbodeaborane was prepared successfully.

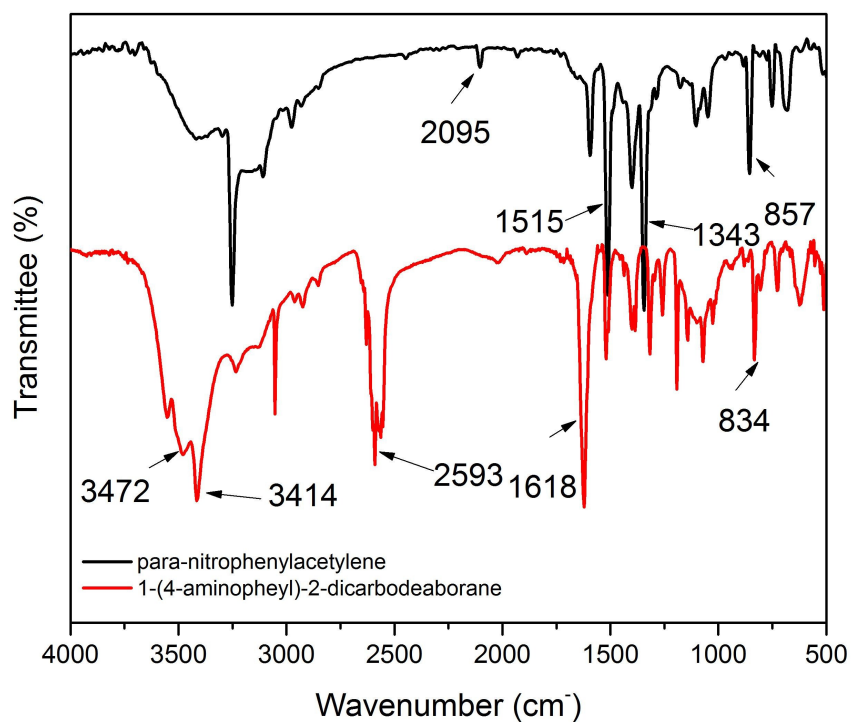
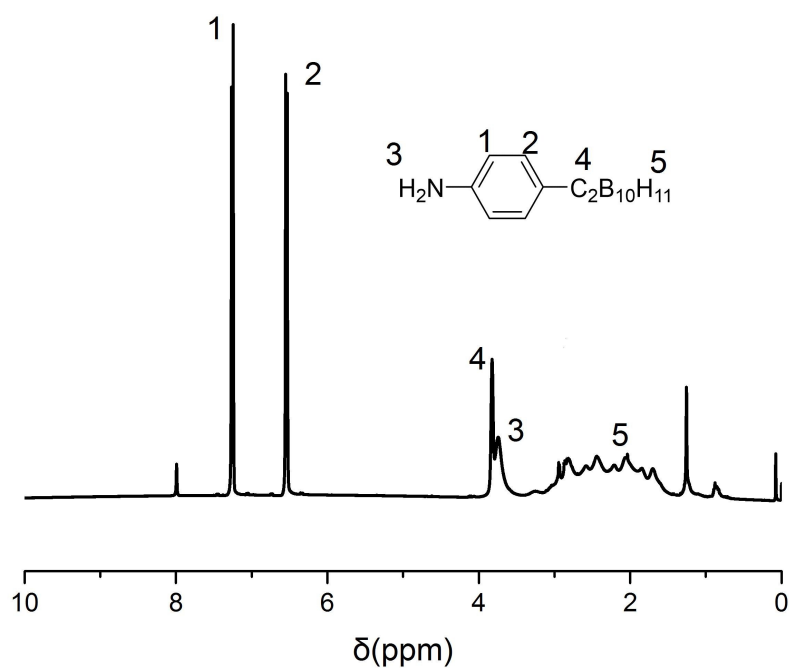


Figure 2. FTIR spectrum of para-nitrophenylacetylene and 1-(4-aminophenyl)-2-dicarbodeaborane



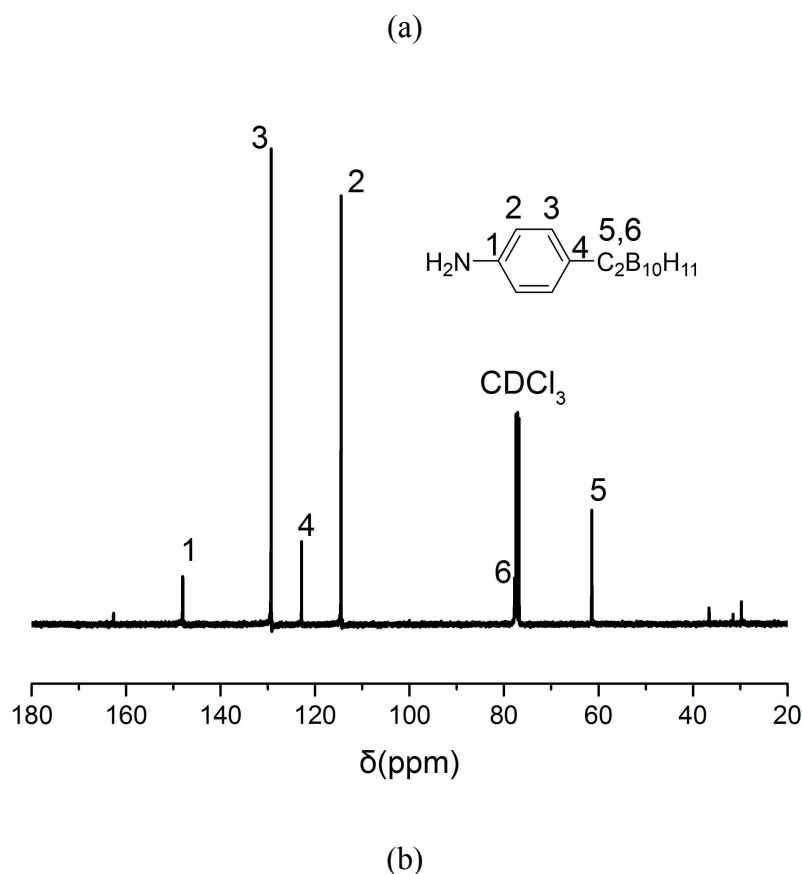


Figure 3.  $^1\text{H}$ -NMR (a) and  $^{13}\text{C}$ -NMR (b) of compound 2

### Characterization of AFR-PEPA and Carb-PEPA

The chemical structures of AFR-PEPA and Carb-PEPA before and after thermal curing at  $380^\circ\text{C}/1\text{h}$  were determined by FTIR. The results are shown in Figure 4. The absorptions around  $1726\text{ cm}^{-1}$  and  $1785\text{ cm}^{-1}$  are attributed to the symmetric and asymmetric stretching of imide  $\text{C}=\text{O}$  bond, respectively. The adsorption band at  $2210\text{ cm}^{-1}$  corresponds to the characteristic band of triple bond  $\text{C}\equiv\text{C}$ , indicating alkyne groups embedded in the imide chains are stable during the imide synthesis and subsequent drying process. However, this peak is absent after thermal curing, indicating that the phenylethynyl groups were involved in the cure reactions.

Compared to AFR-PEPA, the characteristic absorption peak around  $2600\text{ cm}^{-1}$  for Carb-PEPA is resulted from the stretching of B-H, which can be still observed clearly after curing.

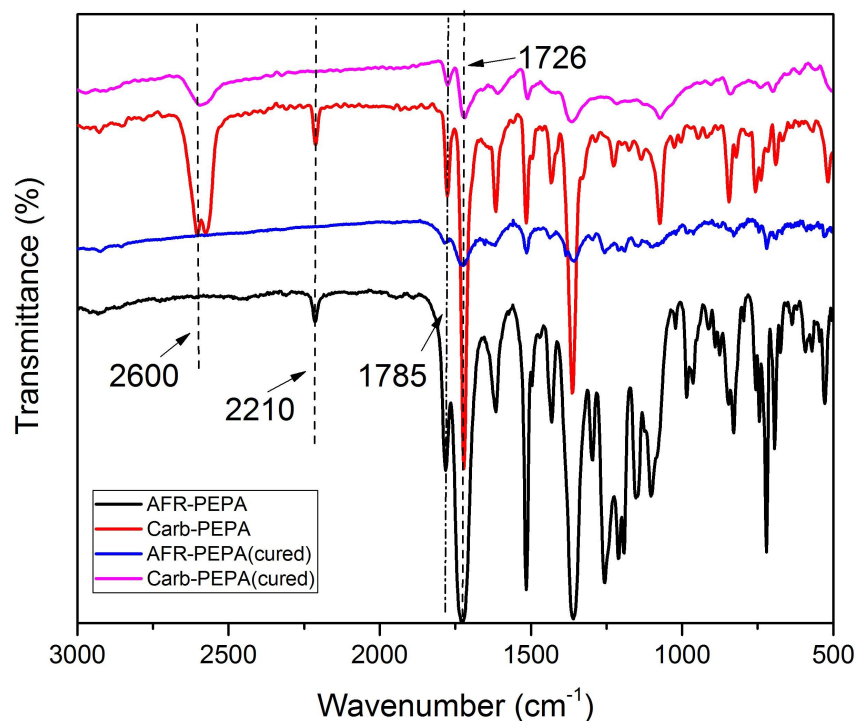


Figure 4. FTIR spectra of AFR-PEPA and Carb-PEPA before and after curing

Figure 5 shows the  $^1\text{H-NMR}$  results of Carb-PEPA in  $\text{CDCl}_3$ . All of the protons in Carb-PEPA were detected as expected, confirming that the imide compound was synthesized successfully.

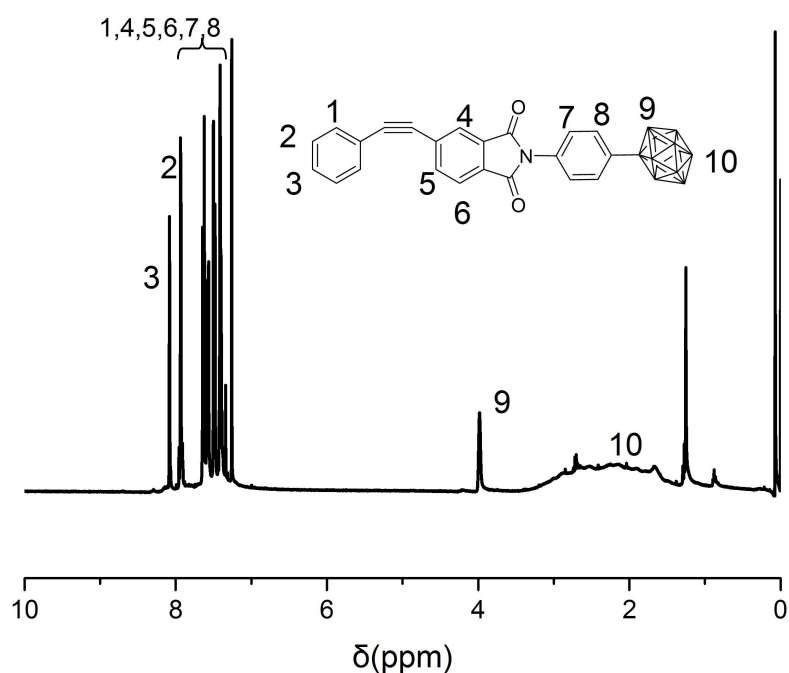


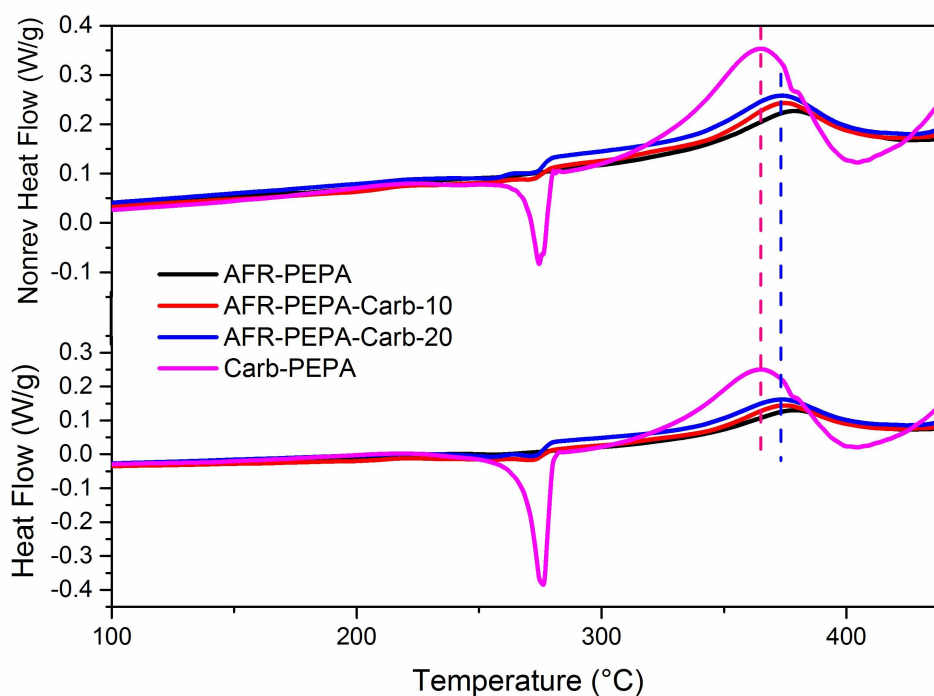
Figure 5. <sup>1</sup>H-NMR of Carb-PEPA

### Thermal cure of imide systems

Thermal curing of imide systems was examined by MDSC. The advantages of MDSC are its increased sensitivity to small transitions, enabling the separation of a number of overlapping thermal events, as well as the separation of reversing and non-reversing heat flow within one single measurement. 【24】 The thermograms and relevant thermal parameters are shown in Figure 6 and Table 1 respectively. A melting peak around 278°C in the MDSC curves indicates the presence of crystalline structure in the Carb-PEPA. With the addition of Carb-PEPA into AFR-PEPA, an endothermic peak can be observed in the range of 260-280°C for the imide blends. The broad exothermic peaks in the range of 330-420°C are attributed to the thermal curing

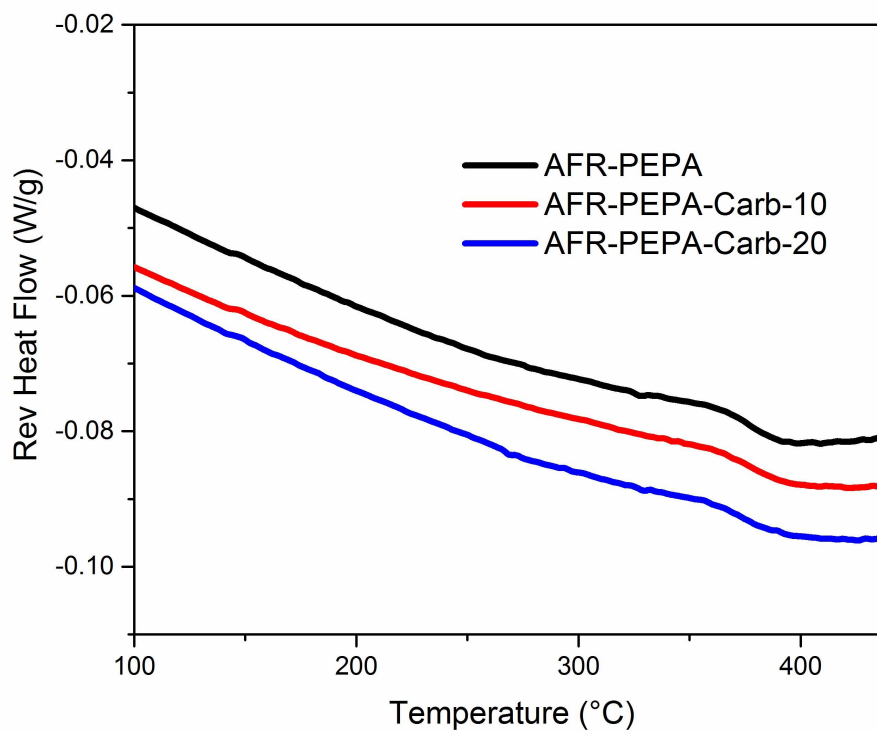
reaction of phenylethynyl groups in the main chains. It can be seen in Figure 6 that the values of cure peak temperature from non-reversing heat flow are almost the same with those from total heat flow.

T<sub>g</sub> of cured polyimides was measured by using MDSC (listed in Table 1). It can be seen that T<sub>g</sub> of cured polyimides increases with the increasing of Carb-PEPA contents in the blends. T<sub>g</sub> of cured AFR-PEPA-Carb-20 is 389.5°C, which is 15°C higher than that of AFR-PEPA. This may be attributed to the remarkable steric hindrance and rigid structure of carborane. 【1】



(a)





(b)

Figure 6. MDSC thermograms of imide samples and cured polyimides. (a) imide samples, (b) cured polyimides.

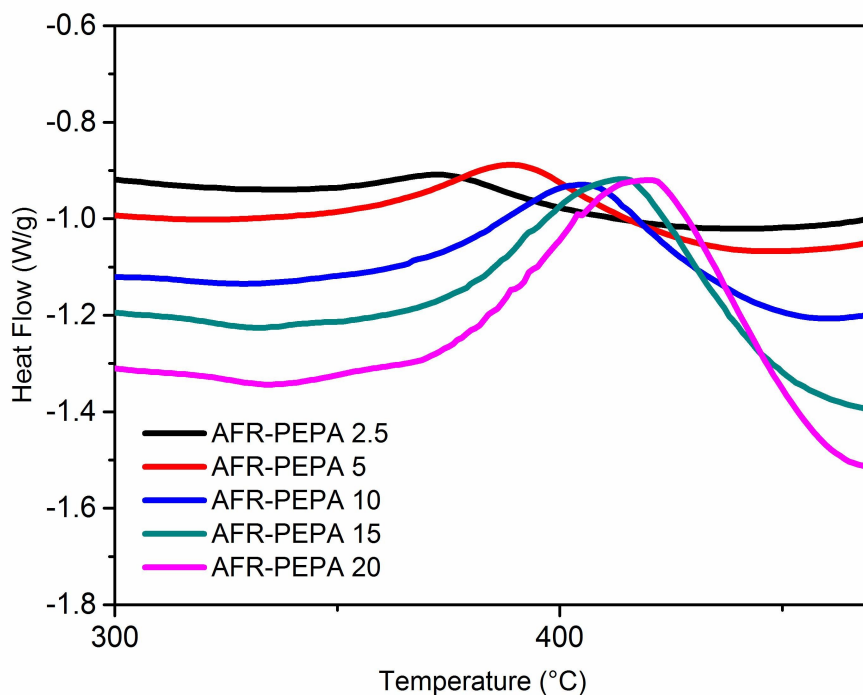
Table 1. MDSC data of imide samples

Sample	T <sub>g</sub> (°C)	ΔH(KJ/mol)
AFR-PEPA	374.0	109.2
AFR-PEPA-Carb10	386.6	105.4
AFR-PEPA-Carb20	389.5	98.2

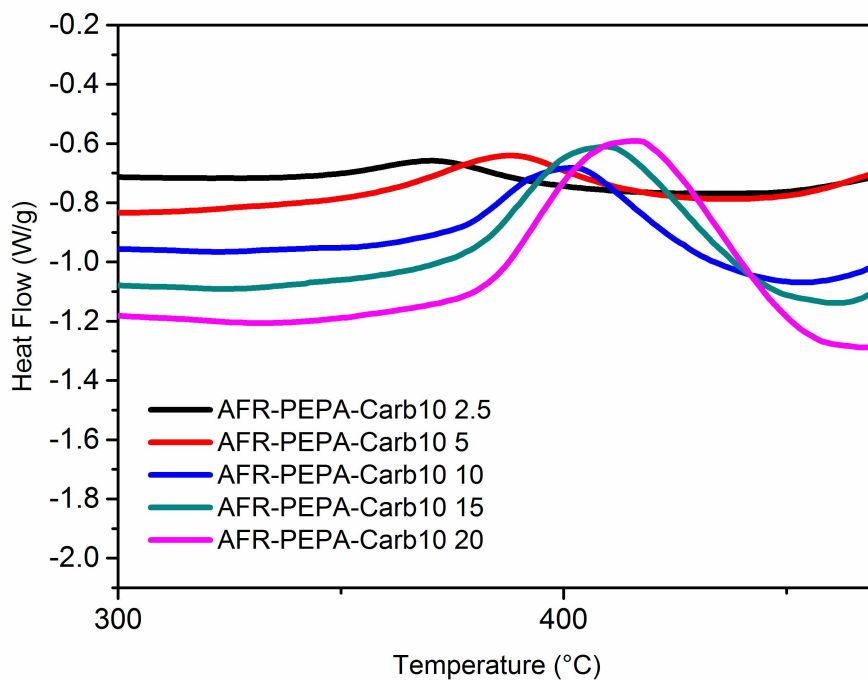
ΔH: the exothermic enthalpy per mole of triple bonds; T<sub>g</sub>: glass transition temperature of cured resins determined by MDSC.

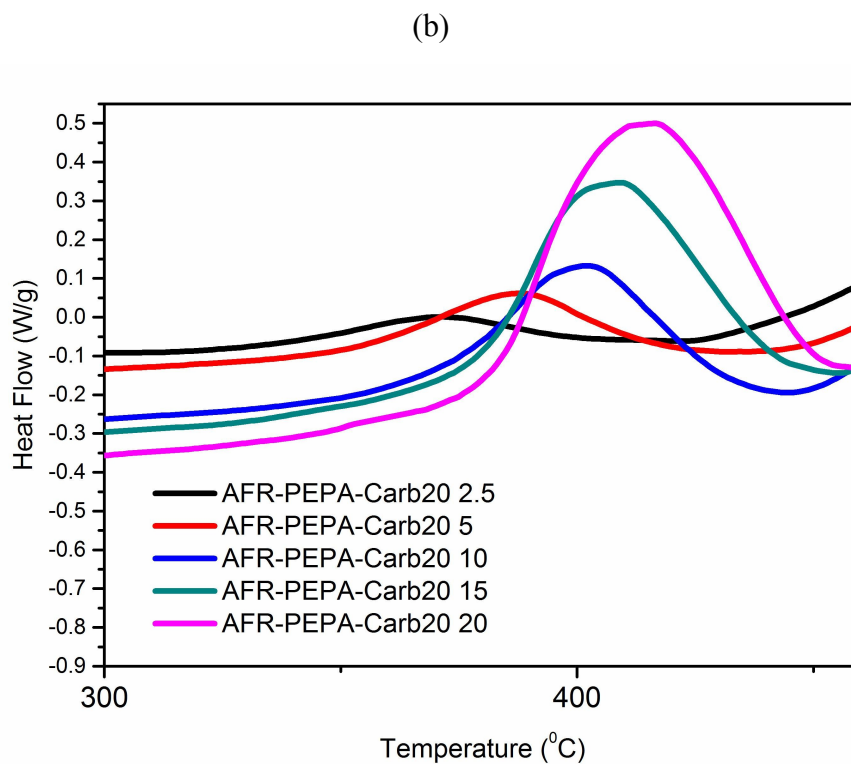
### Non-isothermal cure kinetics of imide systems

In order to better understand the thermal curing reaction and cure kinetics of the obtained imide systems, non-isothermal DSC tests at different heating rates were conducted. The experimental results are shown in Table 2.



(a)





(c)

Figure 7. DSC curves of imide systems at different heating rates. (a). AFR-PEPA. (b).AFR-PEPA-Carb-10. (c). AFR-PEPA-Carb-20

Table 2. DSC data of imide systems at different heating rates

Sample	$\beta$ (°C/min)	Characteristic temperatures			$\Delta T$ (°C)
		$T_i$ (°C)	$T_p$ (°C)	$T_t$ (°C)	
AFR-PEPA	2.5	319.9	373.9	426.1	106.1
	5	322.8	391.2	443.1	120.3
	10	325.6	407.0	459.2	133.6
	15	326.5	415.9	466.3	139.8
	20	331.3	421.6	474.4	143.1
AFR-PEPA-Carb-10	2.5	310.9	372.6	423.7	112.8

	5	320.8	384.8	434.1	113.3
	10	325.6	403.8	455.0	129.4
	15	328.4	410.2	460.6	132.2
	20	333.2	417.2	466.8	133.6
	2.5	317.1	369.3	420.4	103.3
	5	326.1	387.1	433.6	107.6
AFR-PEPA-Carb-20	10	329.3	402.0	446.0	116.7
	15	335.1	404.8	453.9	118.8
	20	348.8	410.6	455.0	106.1

T<sub>i</sub>: initial curing temperature, T<sub>p</sub>: peak temperature, T<sub>t</sub>: terminal temperature;  $\Delta T$ : curing temperature range;  $\beta$ : heating rate

DSC curves of imide systems at different heating rates of 2.5, 5, 10, 15, 20°C/min respectively were showed in Figure 7. It can be seen that the curing peaks become sharper and the cure characteristic temperatures (T<sub>i</sub>, T<sub>p</sub> and T<sub>t</sub>) shift to higher values with increasing heating rates. For example, the T<sub>p</sub> of AFR-PEPA increased from 373.9 to 421.6°C when the heating rate increased from 2.5 to 20°C/min. This can be attributed to the enhanced thermal effect and larger temperature difference at higher heating rates. As a result, the endothermic peak shifts to a higher temperature. Besides,  $\Delta T$  of AFR-PEPA-Carb-20 decreased by 37°C compared to AFR-PEPA at a heating rate of 20°C/min, implying that the introduction of carborane structure could narrow the reaction window for thermal curing of imide systems.

The characteristic temperatures ( $T_i$ ,  $T_p$  and  $T_t$ ) of imide systems are plotted as the function of heating rates, as shown in Figure 8. It can be observed that all the characteristic temperatures increase linearly with increasing heating rates. Furthermore, the characteristic temperatures at a heating rate of  $0^\circ\text{C}/\text{min}$ , corresponding to the pre-curing temperature ( $T_{i0}$ ), constant-curing temperature ( $T_{p0}$ ) and post-curing temperature ( $T_{t0}$ ) respectively, were determined via extrapolation (The results are listed in Table 3). These parameters are very important for optimizing the thermal curing process of imide systems.

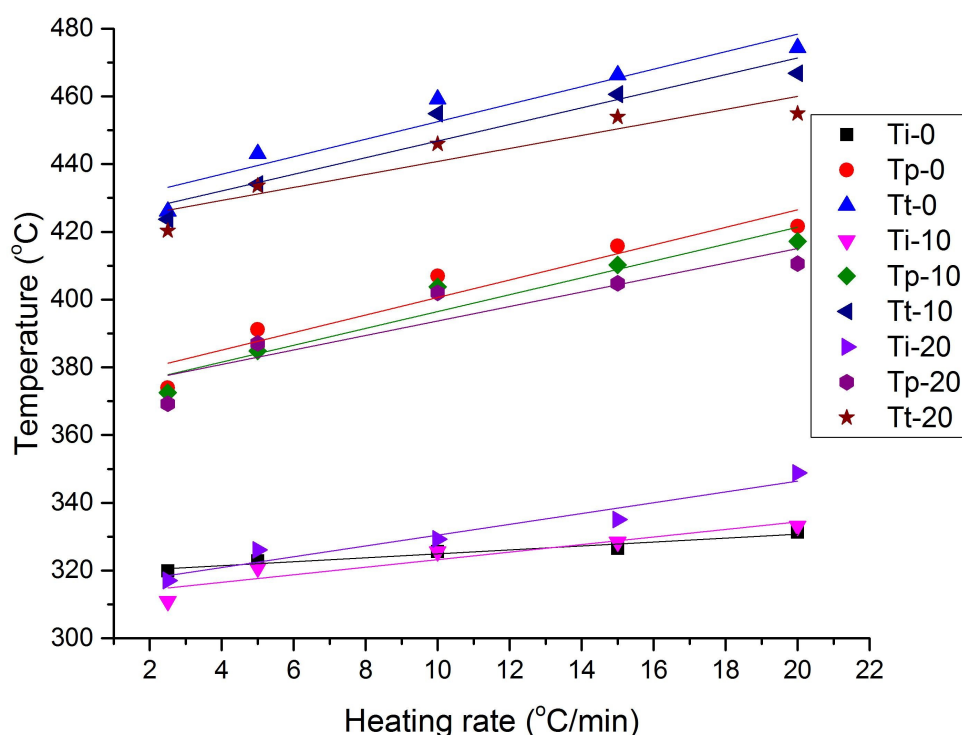


Figure 8. Linear relationship between the heating rates and characteristic temperatures of imide systems.  $T_x-0$  represents the characteristic temperature of AFR-PEPA.  $T_x-10$  represents the characteristic temperature of AFR-EPPA-Carb-10.  $T_x-20$  represents the characteristic temperature of AFR-PEPA-Carb-20 ( $x=i, p, t$ ).

Table 3. Characteristic temperatures of imide systems for curing at 0°C/min.

Sample	T <sub>io</sub> (°C)	T <sub>po</sub> (°C)	T <sub>to</sub> (°C)
AFR-PEPA	319.1	374.7	426.7
AFR-PEPA-Carb-10	312.1	371.6	422.3
AFR-PEPA-Carb-20	314.5	372.3	421.6
Carb-PEPA	298.7	364.1	408.4

T<sub>io</sub>: pre-curing temperature; T<sub>po</sub>: constant-curing temperature; T<sub>to</sub>: post-curing temperature

It can be observed in Table 3 that the characteristic temperatures of imide systems decrease slightly with the addition of Carb-PEPA. It recommends that the curing process of AFR-PEPA imide oligomers should not be significantly influenced by the blending of Carb-PEPA into the systems.

The analysis of curing kinetic for imide systems was performed with Kissinger and Crane methods. 【25-30】

According to Kissinger equation (Equation 1), the activation energy  $E$  can be obtained from the slope of the plots of  $\ln(\beta/T_p^2)$  versus  $1/T_p$ .

$$\frac{d \ln(\beta/T_p^2)}{d(1/T_p)} = -\frac{E}{R} \quad (1)$$

Where  $R$  is the gas constant,  $\beta$  is the heating rate and  $T_p$  is the peak temperature.

The values of  $\ln(\beta/T_p^2)$  and  $1000/T_p$  for the imide systems are shown in Table S1 (ESI †) and plotted in Figure 9. The activation energy  $E$  of AFR-PEPA, AFR-PEPA-Carb-10 and AFR-PEPA-Carb-20 is calculated to be 151.3 KJ/mol,

156.47 KJ/mol and 170.61 KJ/mol, respectively. The higher Carb-PEPA contents in imide blends, the higher the activation energy of the systems. It indicates that Carb-PEPA has a lower reactivity compared to AFR-PEPA.

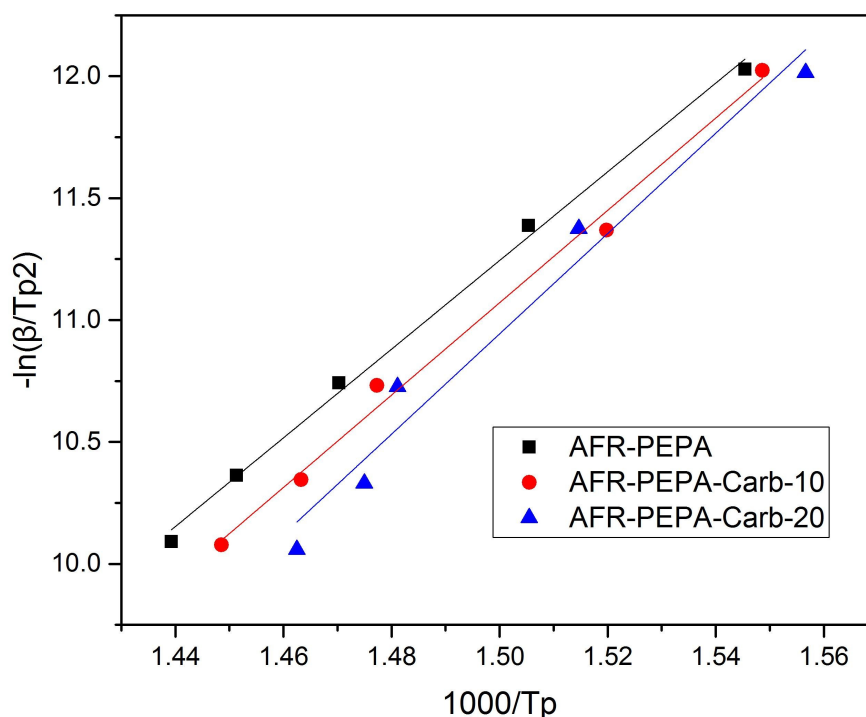


Figure 9. Fitted plots of  $\ln(\beta/T_p^2)$  versus  $1000/T_p$  based on Kissinger equation

According to Crane equation (Equation 2), reaction order  $n$  can be obtained from the slope of the plots of  $\ln\beta$  versus  $1/T_p$

$$\frac{d \ln \beta}{d(1/T_p)} = -\frac{E}{nR} \quad (2)$$

Besides, a frequency factor  $A$  derived from Kissinger equation can be expressed as Equation 3. The frequency factor reflects the effective collisions between reactive groups.

$$A = \frac{\beta E \exp(E/(RT_p))}{RT_p^2} \quad (3)$$

The reaction order  $n$  and frequency factor  $A$  were calculated from Kissinger and

Crane equations. The results are listed in Table 4. It can be seen that the cure reaction of carborane-containing imide blends still follow the first-order kinetics of phenylethynyl-terminated compounds. For the studied imide systems, the increase of activation energy  $E$  is accompanied by a simultaneous increase of frequency factor  $A$ . The activation energy  $E$  is defined as the energy barrier that should be overcome in order to activate a chemical reaction. The introduction of carborane structure in imide oligomers would restrict the mobility of main chains. Therefore, the reactants need to overcome a higher energy barrier, resulting in an increased activation energy for the curing reaction. According to the collision theory, the frequency factor  $A$  reflects the intensity of reactive collisions during the reaction. The reaction rate is proportional to the number of active sites available for chemical reaction. 【31】 Compared with AFR-PEPA imide oligomer, imide compound Carb-PEPA has much more concentrated phenylethynyl groups in its chemical structure. Therefore, the introduction of Carb-PEPA in imide systems facilitates to the formation of more active sites, resulting in more intensive collision between phenylethynyl groups and higher frequency factor  $A$ . For example, the frequency factor  $A$  of AFR-PEPA-Carb-20 increased by one order of magnitude compared to AFR-PEPA. M.E. Wright et al. 【32, 33】 synthesized and studied the thermal cure kinetics of arylethynyl terminated polyhedral oligomeric silsesquioxane (POSS) containing imide oligomers. Similar to Carb-PEPA, the presence of POSS could also increase both the activation energy  $E$  and frequency factor  $A$  of the cure reaction of imide oligomers.



Table 4. The kinetic parameters of the cure reaction of imide systems

Sample	$E$ (KJ/mol)	$A$ (s-)	$n$
AFR-PEPA	151.15	$1.66 \times 10^{11}$	0.93
AFR-PEPA-Carb-10	157.47	$6.43 \times 10^{11}$	0.93
AFR-PEPA-Carb-20	171.02	$9.21 \times 10^{12}$	0.94
Carb-PEPA	161.71	$2.15 \times 10^{12}$	0.94

If the thermal cure of the material follows the  $n$ th-order kinetics, the rate of cure reaction  $d\alpha/dt$  is usually expressed as the following equation:

$$\frac{d\alpha}{dt} = A \exp\left(-\frac{E}{RT}\right)(1-\alpha)^n \quad (4)$$

Where  $\alpha$  is the degree of cure,  $(1-\alpha)^n$  is a function of the fractional extent of conversion,  $t$  is the reaction time,  $d\alpha/dt$  is the rate of conversion.

Thus, the curing behavior of the imide systems can be described by the following reaction rate equations based on the data listed in Table 4. The relationship of conversion  $\alpha$  versus time at different cure temperatures were plotted according to the following equations and presented in supporting information.

For AFR-PEPA:

$$\frac{d\alpha}{dt} = 1.66 \times 10^{11} \exp\left(-\frac{151150}{RT}\right)(1-\alpha)^{0.93}$$

For AFR-PEPA-Carb-10:

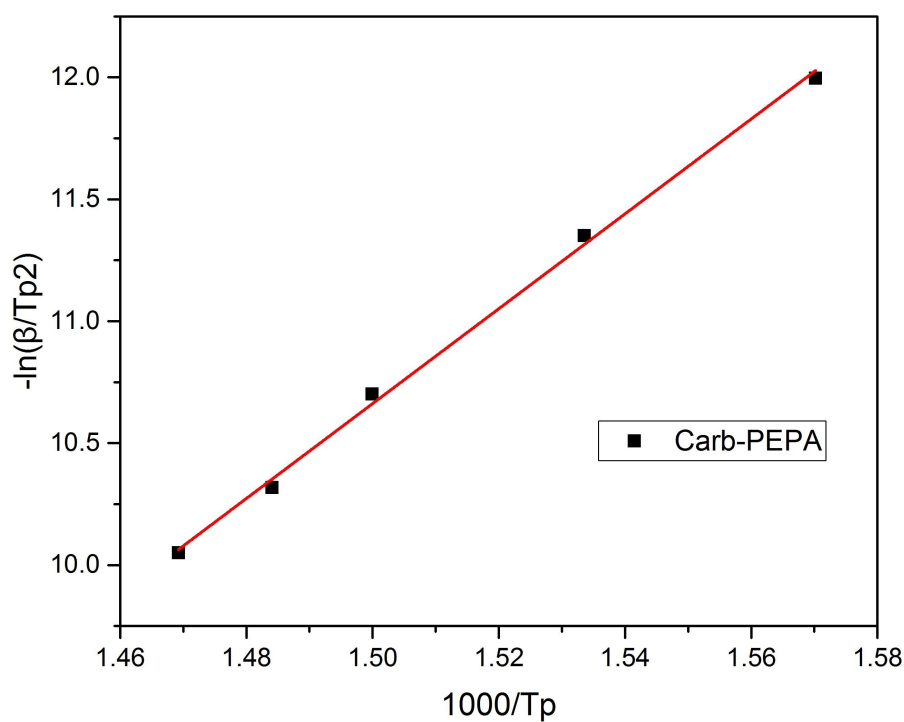
$$\frac{d\alpha}{dt} = 6.43 \times 10^{11} \exp\left(-\frac{157450}{RT}\right)(1-\alpha)^{0.93}$$

For AFR-PEPA-Carb-20:

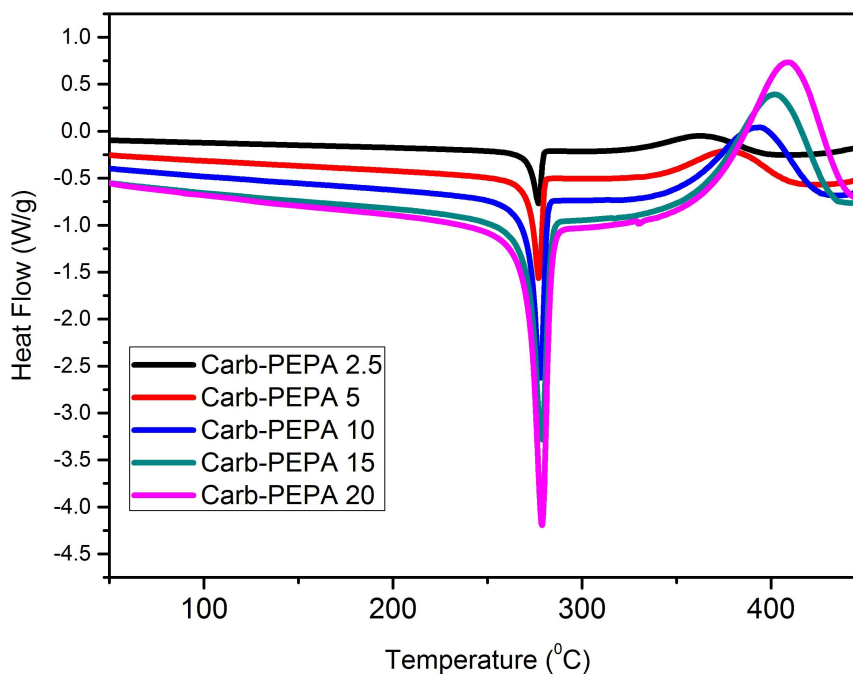
$$\frac{d\alpha}{dt} = 9.21 \times 10^{12} \exp\left(-\frac{171020}{RT}\right)(1-\alpha)^{0.94}$$

### Non-isothermal cure kinetics of imide compound Carb-PEPA

In order to better understand the effect of Carb-PEPA on the curing reaction of the resin systems, the curing behavior of the imide compound Carb-PEPA itself was further investigated. The DSC curves and Kissinger plot of the model compound are shown in Figure 10, and the relevant data are listed in Table 5.



(a)



(b)

Figure 10. The Fitted Kissinger plot (a) and DSC curves (b) of Carb-PEPA at different heating rates

Compared with AFR-PEPA imide oligomer, the imide compound Carb-PEPA has much more concentrated phenylethynyl groups in its chemical structure. Figure 10b shows the dynamic DSC curves of the curing reaction of Carb-PEPA at different heating rates of 2.5, 5, 10, 15, 20°C/min, respectively. All the DSC curves of Carb-PEPA present sharp melting peaks at 278°C. Using the same procedure mentioned earlier, the activation energy  $E$ , reaction order  $n$  and frequency factor  $A$  were calculated. The results are listed in Table 4.

The activation energy  $E$  of Carb-PEPA is 161.71 KJ/mol, which is higher than that of AFR-PEPA. Y. Li and B. Securer **【23, 25】** also reported that the values of activation energy  $E$  of monofunctional phenylethynyl compounds are higher than that of

bifunctional ones. However, the imide blend AFR-PEPA-Carb-20 has a higher  $E$  values than Carb-PEPA. The carborane could restrict the mobility of main chains of AFR-PEPA so that AFR-PEPA-Carb-20 needs to overcome a higher energy barrier for the curing reaction. The curing behavior of Carb-PEPA can be described by the following equation:

$$\frac{d\alpha}{dt} = 2.15 \times 10^{12} \exp\left(-\frac{161710}{RT}\right)(1-\alpha)^{0.94}$$

Li and Morgan [23] studied the thermal reaction of AFR-PEPA and a model compound N-phenyl-[(4-phenylethynyl) phthalimide]. Two-stage kinetic/diffusion model could explain the curing process of AFR-PEPA or N-phenyl-[(4-phenylethynyl) phthalimide] effectively. However, compared with the N-phenyl-[(4-phenylethynyl) phthalimide], the imide compound Carb-PEPA has a much larger molecular structure so that ethynyl to ethynyl addition would be the dominant reaction during thermal cure due to the steric hindrance of carborane. Other kinds of addition reactions such as the Diels-Alder cycloaddition would barely happen. The proposed cure reactions in the Carb-PEPA and AFR-PEPA/Carb-PEPA imide blends are shown in Figure 11 and 12 respectively.

Table 5. The DSC data of Carb-PEPA at different heating rates

Sample	$\beta$ (°C/min)	Characteristic temperatures			$\Delta T$ (°C)
		Ti(°C)	Tp(°C)	Tt(°C)	
Carb-PEPA	2.5	290.5	363.7	408.0	117.5
	5	311.9	378.9	423.7	111.8

---

10	316.1	393.5	434.6	118.5
15	310.0	400.7	442.6	132.7
20	316.1	407.5	450.2	134.1

---

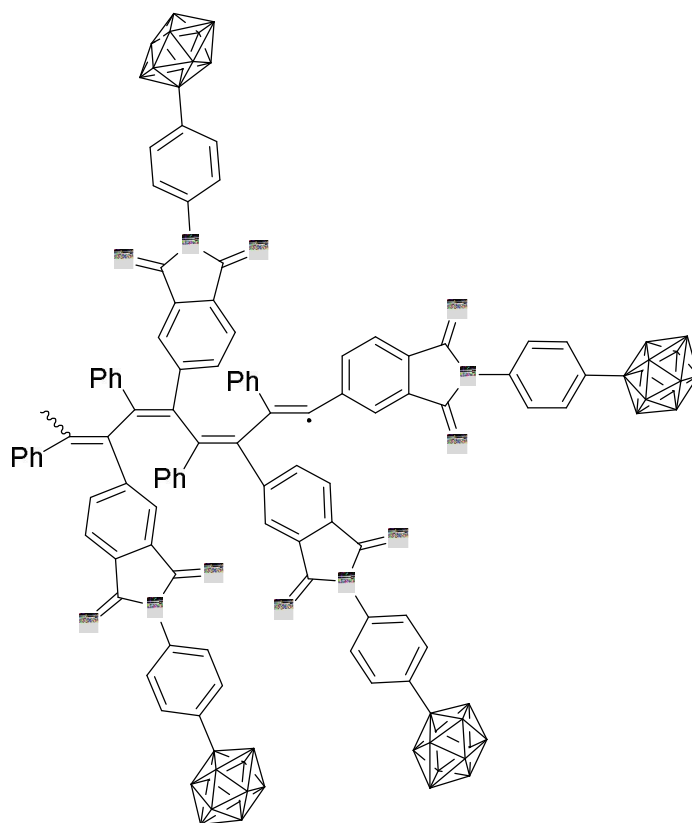


Figure 11. Proposed cure reactions of Carb-PEPA

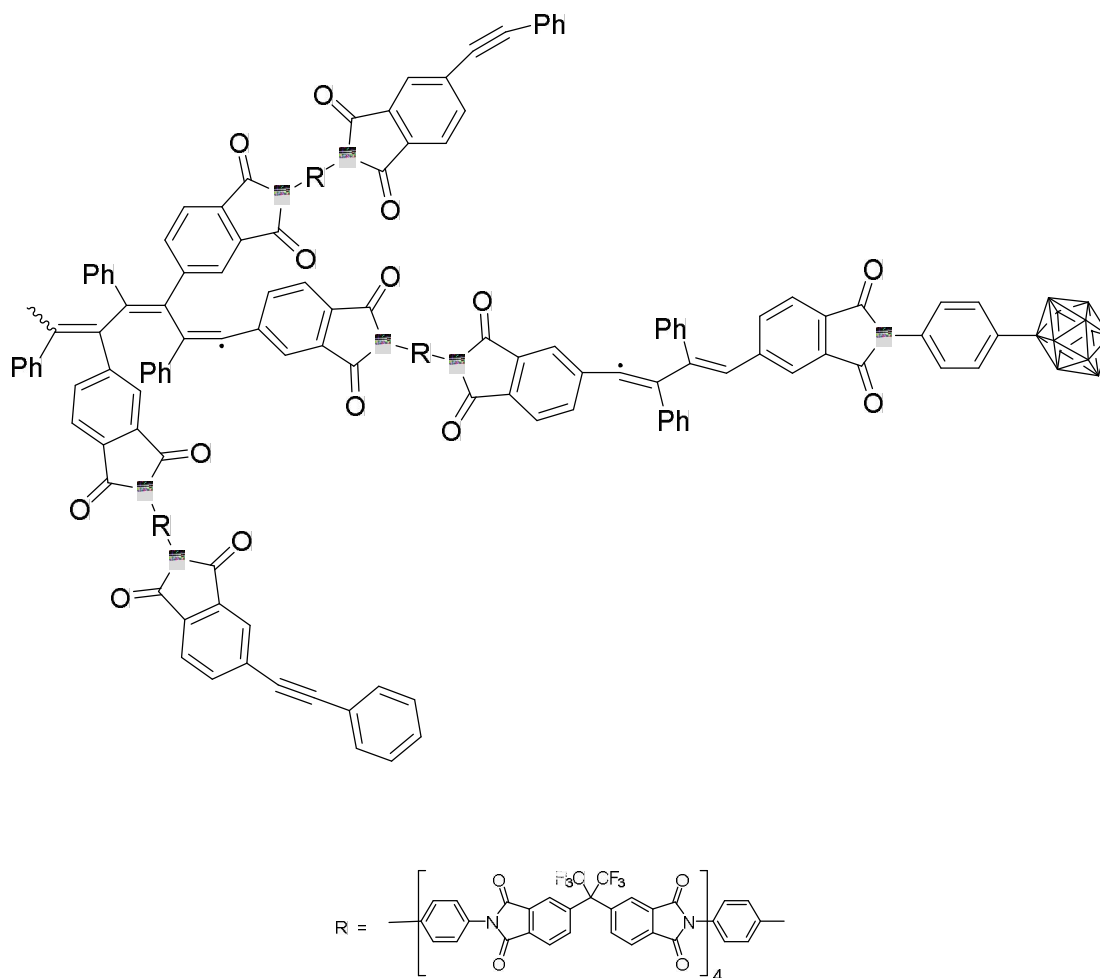


Figure 12. Proposed cure reactions of AFR-PEPA/Carb-PEPA imide blends

### Thermal stability of the imide systems

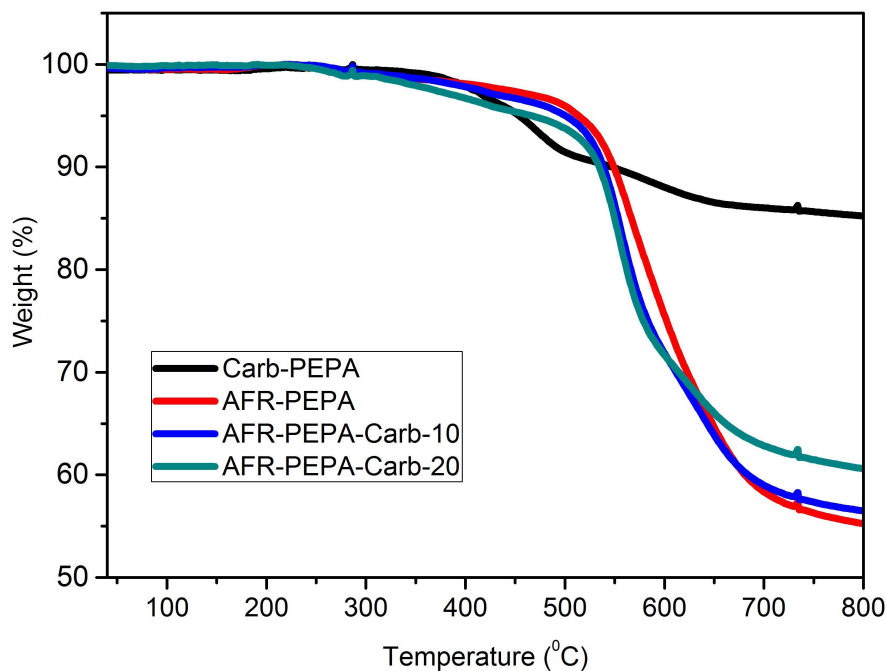


Figure 13. TGA curves of the imide systems under nitrogen atmosphere

Table 6. TGA data of imide systems

Sample	$T_{5\%}(\text{°C})$	$T_{10\%}(\text{°C})$	$WL_{500-800}(\text{°C})$	Char Yield at 800°C
				(%)
Carb-PEPA	453.7	546.7	6.3	85.2
AFR-PEPA	513.3	548.6	40.7	55.2
AFR-PEPA-Carb-10	500.3	538.7	38.5	56.5
AFR-PEPA-Carb-20	466.3	534.3	33.2	60.6

$T_{5\%}$ : temperature for 5% weight loss;  $T_{10\%}$ : temperature for 10% weight loss

$WL_{500-800}$ : the weight loss between 500°C and 800°C

The thermal stability of carborane-containing imide systems was characterized by

TGA under nitrogen atmosphere. The resultant TGA curves are shown in Figure 13. The temperature for 5% ( $T_{5\%}$ ) and 10% ( $T_{10\%}$ ) weight loss and the char yield at 800°C are listed in Table 6. Both AFR-PEPA-Carb-10 and AFR-PEPA-Carb-20 exhibit lower  $T_{5\%}$  and  $T_{10\%}$  together with higher char yield at 800°C than AFR-PEPA due to the introduction of carborane in the system. By way of example, the  $T_{5\%}$  of AFR-PEPA-Carb-20 decreased by around 47°C compared to AFR-PEPA, while the corresponding char yield at 800°C increased from 55.2% to 60.6%.

It can be also seen in Table 6 that  $T_{5\%}$  and  $T_{10\%}$  of Carb-PEPA are lower than those of AFR-PEPA. At around 470°C there is an obvious weight loss of Carb-PEPA due to the pyrolysis of carborane groups. 【17】 However, the char yield of Carb-PEPA is extremely high, which reaches 85.2% at 800°C. It could be attributed to the presence of a passivation layer with oxidized carborane formed on sample's surface to prevent further erosion. 【1】

## Conclusion

A novel carborane-containing imide compound Carb-PEPA was synthesized and used as a modifier to improve the thermal properties of AFR-PEPA. The structure of the products was confirmed by  $^1\text{H-NMR}$ ,  $^{13}\text{C-NMR}$  and FTIR spectroscopy. The imide system containing 20 wt% Carb-PEPA (AFR-PEPA-Carb-20) exhibits the highest glass transition temperature (389.5°C) due to high steric hindrance of carborane. The thermal cure kinetics of the imide systems was studied by DSC and analyzed with Kissinger method. The results show that the curing reaction of the resin systems agrees with the first-order reaction. Both the activation energy  $E$  and frequency  $A$  for



the imide oligomers increase with the addition of Carb-PEPA. The residual weight ratios of the resin systems under nitrogen also increase with the addition of Carb-PEPA. A high char yield (60.6%) at 800°C for the AFR-PEPA-Carb-20 can be attributed to the incorporation of carborane cage structures and the formation of a protective layer during thermal degradation. This work presents a simple and efficient method to develop high-performance organic/inorganic hybrid polyimide resins.

### Acknowledgments

This work was financially supported by the National Natural Science Foundation of China (No. 51173152) and Scientific Research Innovation Team (2013XJZT005) of Southwest Petroleum University.

### References

1. X. Huang, Q. Zhang, Z. Meng, J. Gu, X. Jia and K. Xi, *J. Polym. Sci. Part A: Poly. Chem.*, 2015, 53, 973-980.
2. Q. Zhou, Z. Mao, L. Ni and J. Chen, *J. Appl. Polym. Sci.*, 2007, 104, 2498-2503.
3. M. Yang, D. Wang, N. Sun, C. Chen and X. Zhao, *High. Perform. Polym.*, 2014, 27, 449-457.
4. X. Meng, J. Yan, W. Fan, J. Liu, Z. Wang and G. Li, *RSC Adv.*, 2014, 4, 37458-37469.
5. C. Liu, X. Zhao, X. Yu, W. Wang, H. Jia, Y. Li, H. Zhou and C. Chen, *Polym.*

- Degrad. Stabil.*, 2013, 98, 230-240.
6. H. Kimura, *Express. Polym. Lett.*, 2012, 7, 161-171.
  7. Y. Yang, L. Fan, X. Qu, M. Ji and S. Yang, *Polymer*, 2011, 52, 138-148.
  8. C. n. Su, M. Ji, L. Fan and S. y. Yang, *High. Perform. Polym.*, 2011, 23, 352-361.
  9. T. K. Minton, M. E. Wright, S. J. Tomczak, S. A. Marquez, L. Shen, A. L. Brunsvold, R. Cooper, J. Zhang, V. Vij, A. J. Guenther and B. J. Petteys, *ACS. Appl. Mater. Inter.*, 2012, 4, 492-502.
  10. D. M. Pinson, G. R. Yandek, T. S. Haddad, E. M. Horstman and J. M. Mabry, *Macromolecules*, 2013, 46, 7363-7377.
  11. J. E. Lincoln, R. J. Morgan and D. B. Curliss, *Polym. Composite.*, 2008, 29, 585-596.
  12. J. E. Lincoln, S. Hout, K. Flaherty, D. B. Curliss and R. J. Morgan, *J. Appl. Polym. Sci.*, 2008, 107, 3557-3567.
  13. D. Xiang, E. Harkin-Jones and D. Linton, *RSC Adv.*, 2015, 5, 47555-47568.
  14. D. Xiang, E. Harkin-Jones and D. Linton, *RSC Adv.*, 2014, 4, 44130-44140.
  15. H. Zhou, Q. Zhou, Q. Zhou, L. Ni and Q. Chen, *RSC Adv.*, 2015, 5, 12161-12167.
  16. M. A. Fox and K. Wade, *J. Mater. Chem.*, 2002, 12, 1301-1306.
  17. X. Men, Y. Cheng, G. Chen, J. Bao and J. Yang, *High. Perform. Polym.*, 2014, 27, 497-509.
  18. R.N. Grimes. *Carboranes*. 2<sup>nd</sup> edition, Oxford: Academic Press, 2011
  19. D. A. Brown, H. M. Colquhoun, J. A. Daniels, J. A. H. MacBride, I. R. Stephenson and K. Wade, *J. Mater. Chem.*, 1992, 2, 793-804.

20. T. Xing, Y. Huang, K. Zhang and J. Wu, *RSC Adv.*, 2014, 4, 53628-53633.
21. P. R. Serwinski and P. M. Lahti, *Org. Lett.*, 2003, 5, 2099-2102.
22. B. P. Dash, R. Satapathy, E. R. Gaillard, K. M. Norton, J. A. Maguire, N. Chug and N. S. Hosmane, *Inorg. Chem.*, 2011, 50, 5485-5493.
23. Y. Li and R. J. Morgan, *J. Appl. Polym. Sci.*, 2006, 101, 4446-4453.
24. D. K. Chouhan, S. K. Rath, A. Kumar, P. S. Alegaonkar, S. Kumar, G. Harikrishnan and T. U. Patro, *J. Matter. Sc.*, 2015, 50, 7458-7472.
25. B. Securer, V. Vij, T. Haddad, J.M. Mabry and A. Lee, *Macromolecules*, 2010, 43, 9337-9347
26. J. Sun, W. Wei, Y. Xu, J. Qu, X. Liu and T. Endo, *RSC Adv.*, 2015, 5, 19048-19057.
27. H.-W. Cui, K. Suganuma and H. Uchida, *RSC Adv.*, 2015, 5, 2677-2683.
28. Z. Zhou, A. Li, R. Bai and J. Sun, *Polym. Composite.*, 2014, 35, 596-601.
29. L. Xia, X. Zhai, X. Xiong and P. Chen, *RSC Adv.*, 2014, 4, 4646-4655.
30. D. Tan, T. Shi and Z. Li, *Res. Chem. Intermediat.*, 2011, 37, 831-845.
31. G. Skodras, G. Nenes and N. Zafeiriou, *Appl. Therm. Eng.*, 2015, 74, 111-118.
32. M. E. Wright, D. A. Schorzman, F. J. Feher and R.-Z. Jin, *Chem. Mater.*, 2003, 15, 264-268.
33. M. E. Wright, D. A. Schorzman and A. M. Berman, *Macromolecules*, 2002, 35, 6550-6556.

## Graphical Abstract

JieYue<sup>ab</sup>, Yuntao Li<sup>\*ab</sup>, Hui Li<sup>b</sup>, Yan Zhao<sup>c</sup>, ChunxiaZhao<sup>b</sup>, and XiangyuWang<sup>b</sup>

The thermal behavior of novel carborane-containing phenylethynyl terminated imide model compound and resultant resin systems was studied in this paper.

